ISSN 1995-0780, Nanotechnologies in Russia, 2011, Vol. 6, Nos. 5–6, pp. 311–322. © Pleiades Publishing, Ltd., 2011.
Original Russian Text © T.E. Grigor'ev, E.E. Said-Galiev, A.Yu. Nikolaev, M.S. Kondratenko, I.V. Elmanovich, M.O. Gallyamov, A.R. Khokhlov, 2011, published in Rossiiskie Nanotekhnologii, 2011, Vol. 6, Nos. 5–6.

Electrocatalysts for Fuel Cells Synthesized in Supercritical Carbon Dioxide

T. E. Grigor'ev[a]*, E. E. Said-Galiev[a], A. Yu. Nikolaev[a], M. S. Kondratenko[b],
I. V. Elmanovich[b], M. O. Gallyamov[a, b], and A. R. Khokhlov[a, b]
[a] *Nesmeyanov Institute of Organoelement Compounds, Russian Academy of Sciences,*
ul. Vavilova 28, Moscow, 119991 Russia
** e-mail: timgrigo@polly.phys.msu.ru*
[b] *Faculty of Physics, Moscow State University, Moscow, 119991 Russia*

Received July 14, 2010

Abstract—We applied the method of directly depositing an organometallic precursor from a solution in supercritical carbon dioxide on a dispersed carbon substrate surface followed by reduction to obtain a number of electrocatalytic materials in the form of nanoscale platinum particles on dispersed carbon supports (Vulcan XC72r carbon black, acetylene black, nanotubes). The synthesized materials persistently showed a monodisperse size distribution of platinum particles with an average diameter of 2–3 nm, regardless of the substrate nature, and a uniform distribution over the support surface. The synthesized electrocatalysts (ECs) were tested as part of an operating cathode electrode of a phosphoric acid fuel cell (FC) with a PBI matrix. In this case, the membrane–electrode assembly with this cathode showed current–voltage characteristics as good as the reference characteristics achieved with electrodes produced by BASF.

DOI: 10.1134/S1995078011030062

INTRODUCTION

Recently, due to the development of "green chemistry" methods, researchers have shown increasing interest in new approaches to immobilizing nanoscale metal particles on highly developed surfaces of inorganic matrices of different natures, which can find application in solving problems of increasing the activity and stability of catalytic materials for heterogeneous (electro)catalysis. One promising approach is based on the method of impregnation in supercritical media (SCM) or fluids, the mechanism of which is the diffusion of a solution of an organic metal complex soluble in SCM into a high-porous matrix followed by precursor material adsorption on the substrate [1–4]. Among fluids, i.e., diffusate supports, supercritical carbon dioxide (SC CO_2) is most widely used. Its advantages over conventional liquid solvents are as follows: spontaneous and complete evaporation after the process termination, hence, the elimination of the residual solvent; the absence of any negative effect on catalytic materials (poisoning); a density close to that of liquids (with which the significant solvency for organic precursors of metals is associated); and a viscosity close to that of gases (which presupposes good transport properties). The principal advantage of solutions in SCM is the absence of effects caused by surface tension (such as capillary ones), which provides the absolute penetrability of such a solution into pores of different chemical natures; i.e., it allows uniform wetting and the filling of any porous, dispersed, and rough structures with complex relief configuration. Thus, it becomes possible to perform the uniform transport and adsorption of a precursor material from a solution in SC CO_2 over the entire inner surface of open pores. In this case, the small size of the CO_2 molecule and high mobility of this medium in the SC state yield the high penetrability of this fluid into porous matrices at short times to reach equilibrium [2, 3]. After impregnation is complete, during decompression (again due to the absence of capillary effects for a medium in the SC state), the softest conditions of solvent removal (an analogue of the well-known supercritical drying process [5]) take place, which do not only perturb the morphology of the porous matrix itself, but also the homogeneity of the thin precursor film deposited on its walls. Furthermore, advantages such as nonflammability, incombustibility, explosion safety, low price, availability, low critical parameters (T_{cr} = 31.1°C; P_{cr} = 7.38 MPa), and chemical inertness in the absence of catalysts make SC ÑÎ$_2$ additionally attractive for use as a solvent and transport medium when introducing metal precursors followed by their reduction in high-porous inorganic matrices [6, 7].

These properties explain the recent interest of developers of electrocatalysts (ECs) for fuel cells (FCs) to SC CO_2 [8–16]. The application of SC CO_2 as a reactive medium when synthesizing platinum catalytic particles on the carbon support can be characterized by a number of additional advantages. First, the uniform dispersion of hydrophobic carbon supports such as acetylene black, carbon nanotubes, Sibunit, and other carbon materials with high degree of graphitization and, hence, increased (electro)chemical stability in nonpolar SC CO_2 is possible. Here, the abovementioned advantage of SC CO_2 becomes particularly urgent, i.e., the absence of capillary effects (due to the absence of a phase boundary), which will provide the stability of a material on a support, at least at the stage of matrix impregnation with a precursor solution and subsequent solvent removal (there will be no destructive effect of capillary forces, which takes place when using conventional liquid solvents at the drying stage). In combination with the potentially possible (but still requiring additional improvement) technique of the "dry deposition" of an active layer material on electrodes, where catalytic "ink" components are dispersed and deposited on the electrode surface from SC CO_2 rather than from a liquid medium, this opens up radically new prospects for developing highly stable electrocatalytic materials which ideally fulfill the requirements imposed by adverse (electro)chemical conditions of the FC operation mode, especially for the intermediate-temperature FC with phosphoric acid electrolyte in a polymer (polybenzimidazole (PBI)) matrix on the EC properties.

Despite the active study of systematic features of the synthesis in SC CO_2 and properties of obtained ECs on carbon supports [8–16], question of, e.g., the dependence of the cluster sizes and their distribution on the metal loading, the conditions for achieving a uniform distribution of metal particles over the support surface, the features of the interaction of metal particles with the surface of various supports, the factors controlling the metal cluster size stability during the operation of electrodes on their basis in a phosphoric acid medium, decay decomposition mechanisms of acetylacetonate and fluoroacetylacetonate ligands during metal reduction and methods for removing decomposition products have not been adequately described in the literature. Furthermore, there are no examples of applications of ECs produced using SC technologies in practically operating electrochemical devices. This paper is devoted to the study of structural features and properties of ECs synthesized in the SC CO_2 medium (in comparison with conventional commercial samples) and the direct testing of the produce material incorporated in the cathode electrode of the phosphoric acid FC with a polymer matrix operating at a temperature of 160°C.

EXPERIMENTAL

Materials and Reagents

As a dispersed carbon support for ECs, we chose two black types, i.e., acetylene black AS1 (produced on the experimental setup of the VNIIGAS Open Company, Russia) and carbon black Vulcan XC-72R (produced by the Cabot Corp., United States), as well as baytubes C 150 HP carbon nanotubes delivered by Bayer MaterialScience (Germany). Carbon support materials differ in that acetylene black AS1 and nanotubes are more hydrophobic than Vulcan XC72r; in contrast to Vulcan XC72r black, it is difficult to homogeneously disperse them in aqueous media without additional surface oxidation or without using dispersion stabilizers (e.g., surfactants). The specific surface area of acetylene black AS1 was in the range of 120–150 m^2 g^{-1}, according to measurements by the Brunauer–Emmet–Teller (BET) isotherm method using the Quantochrom NOVA 220e device (Quantochrome Instruments). Carbon black Vulcan XC72R is more hydrophilic, since it is more oxidized (contains polar groups on the surface) and has a larger specific surface area of 210–250 m^2 g^{-1}.

As an EC precursor, we chose a platinum organic complex (1,5-cyclooctadiene) dimethylplatinum (II) (commercial product $C_8H_{12}Pt\,(CH_3)_2$ [COD $Pt(CH_3)_2$], MM = 333 g/mol), with a Pt weight content of ~58% (Aldrich, # 409049). The choice of the precursor was dictated by its appreciable solubility in SC CO_2 ($\sim 4.76 \times 10^{-2}$ mol/l at 80°C and 27.6 MPa [9, 10]). Indeed, the simplest inorganic derivatives of platinum, i.e., platinum hydrochloric acid (H_2PtCl_6), platinum oxides and sulfides (PtO_2 and PtS_2) are insoluble in SC CO_2, and only the commercial organic derivative, i.e., platinum acetylacetonate Pt $(C_5H_7O_2)_2$[Pt $(acac)_2$] has a relatively low solubility in SC CO_2, $\sim 0.4 \times 10^{-5}$ mol/l.

Synthesis Technique

The EC synthesis consists of two stages: (i) impregnation of the carbon matrix with complex and (ii) metal reduction.

(i) In impregnation, a carbon material (powder) and organometallic complex (powder) are loaded into a reactor. They are can be spatially separated or mixed. Then the reactor is made air-tight and CO_2 is puffed at a cylinder pressure (55–60 atm) and heated to a set temperature of 120°C.

Then, using a cylindrical press (High Pressure Equipment Co.), a working pressure of 25 MPa is created and, using a system of valves and capillaries, liquid CO_2 is transported into the reactor and heated above the fluid critical point, where it is transformed to a supercritical state. The press and reactor pressures are measured by manometers. The temperature is maintained using a water or silicon bath mounted on a RET basic C (IKA-WERKE, Germany) heating magnetic mixer with an IKATRON ETS-D5 temperature sensor incorporated into the mixer electronic circuit (the temperature control accuracy is ±0.5°C). The pressure measurement accuracy is ±0.1 MPa.

After exposure with mixing, within a specified time frame (we chose 6 h), at working pressure (25 MPa) and temperature (120°C), the reactor is cooled, depressurized, and carbon black with deposited precursor is removed. At this stage, the control testing of a material could be performed (e.g., by SAXS, elemental analysis, and other methods).

(ii) Metal reduction, in principle, can be performed by a thermal or chemical method using special materials, i.e., reducers. For a high-thermal-stability carbon matrix, thermal reduction can be used, which is what was done in this study; however, since metal clusters on the substrate tend to coarsen with temperature, reduction in a hydrogen flow seems very promising as well. Apparently, this can make it possible to significantly lower the reduction temperature and hence, decrease the sizes of obtained metal particles.

Black materials are highly dispersed powders formed by chain aggregates of nanoscale carbon particles (about several tens of nm in diameter), between which a free porous space is formed. Since carbon black at the impregnation stage in the reactor is uniformly impregnated with a complex solution (rather than dispersion) in SC CO_2, in the case of the nonperturbative removal of the latter, the formation of hyperfine ultrathin homogeneous precursor films adsorbed over the entire surface of dispersed black particles can be expected. During the thermal reduction of adsorbed precursor films in a ÑÎ$_2$ or inert gas atmosphere (or chemical reduction in a hydrogen atmosphere) due to the high surface energy of metal platinum against the background of the low energy of its interaction with the carbon substrate and the low surface energy of the substrate itself, rounded metal platinum particles are formed which poorly "wet" the substrate surface and are nucleation centers for reduced metal. The activity of the obtained electrocatalytic material per platinum mass unit is strongly controlled by the sizes of such particles, although other factors can also have an effect (the local packing period of platinum atoms on the particle surface [17], the structure defect density of metal particles [18], the degree of their mutual coalescence due to agglomeration [19], and others). In general, synthesis using SC CO_2 makes it possible to obtain highly dispersed clusters from several to several tens of nanometers in size depending on the metal type, matrix properties, pressure, and temperature. The deposited precursor film thickness can be varied by impregnation parameters; thus, the metal content on the support surface (loading) and (or) synthesized particle sizes can be controlled.

Upon the completion of the metal reduction stage and the production of nanoscale particles of platinum on carbon black, ligand decomposition products are removed by pumping in vacuum (5–10 Torr, 100–140°C, 6 h).

METHODS FOR TESTING THE SYNTHESIZED EC STRUCTURE TRANSMISSION ELECTRON MICROSCOPY

The transmission electron microscopy (TEM) study was performed as follows. Dispersed particles of the carbon substratum with deposited metal were placed on a formvar film substrate according to the standard procedure of sample preparation for studying. Bright-field micrographs were obtained using a LEO912AB (Carl Zeiss, Germany) in a digital format (recording density is 2048 × 2048 dots) and analyzed using the Femtoscan (Center of Promising Technologies, Russia) adapted software. The data analysis included measurements of platinum particle sizes, a determination of the average particle diameter and its standard deviation, and a calculation of the polydispersity factor and the specific surface area. In this case, the polydispersity factor characterizing the width of the size distribution of particles was determined as the ratio of the weighted average (d_w) and number average (d_n) particle sizes,

$$P \equiv d_w^3/d_n^3 = \frac{\sum_i d_i^3 d_i^3}{\sum_i d_i^3} \Bigg/ \frac{\sum_i d_i^3}{N} = \frac{N\sum_i d_i^6}{\left(\sum_i d_i^3\right)^2}, \qquad (1)$$

where d_i is the measured diameter of the ith particle; summation is performed over all measured values from 1 to $N = 70$ (for all samples, 70 measurements were carried out for particles visualized in several frames). The specific surface area was calculated as the ratio of the total surface of visualized particles to their total mass by the formula

$$S = \frac{6\sum_i d_i^2}{\rho\sum_i d_i^3}, \qquad (2)$$

where ρ is the platinum density (21.45 g/cm^3); summation is also performed over all measured values from 1 to $N = 70$.

X-Ray Diffraction Technique

An X-ray diffraction (XRD) analysis of powders was performed using a Rigaku D/max-RC X-ray diffractometer equipped with a 12-kW radiation source with a rotating anode (graphite analyzing crystal; CuK_α radiation). In view of the small crystallite size and low particle concentration in the carbon matrix, X-raying was performed at a source power close to the maximum one, i.e., $U = 55$ kV, $I = 180$ mA. Diffraction patterns were recorded using the Bragg–Brentano classical focusing scheme.

Electrode Fabrication Technique

The electrode of a phosphoric acid FC with a polymer matrix is a gas-diffusion layer (GDL) on which microporous and active layers are sequentially deposited. The role of the GDL is to provide the free transport of gas reagents, reaction product (water), and electrons. Therefore, a conductive high-porous carbon paper or carbon fabric can be used as a GDL of such FCs. The role of the microporous layer is to increase in reagent flow homogeneity and prevention of GDL flooding by a liquid electrolyte (phosphoric acid) contained in the matrix and partially flooding the active layer. Therefore, the microporous layer is prepared by spraying a mixture of dispersed carbon particles and a hydrophobisator (a fluoropolymer not wettable by water and phosphoric acid; as a rule, highly dispersed polytetrafluoroethylene (PTFE) is used as such). The role of the active layer (AL) is most complex and consists of a stable combination of three transport flows (gas reagents, electrons, and protons) throughout the AL thickness to (from) catalytic centers. To this end, gas channels (open for the free transport of gases) and proton-conducting channels flooded with phosphoric acid (electrolyte) should be combined in the AL structure. Therefore, the active layer is prepared by depositing a mixture of hydrophobisator and dispersed carbon particles with deposited platinum nanoscale clusters. Due to the hydrophobisator distributed over the entire active layer, phosphoric acid, which allows proton transport, fills it only partially (locally), retaining free channels for gas reagent transport.

In this study we used a 280-μm-thick TGP-H-090 (Carbon Fiber Department, Toray Industries Inc.) product as a GDL substrate. Carbon paper itself was not subjected to any hydrophobization. To obtain the GDL, a microporous layer containing 60 wt % of Vulcan XC72r (Cabot) carbon black and 40 wt % of dispersed PTFE (Aldrich, #430935, particle size 1 μm) was deposited on the paper by spraying from dispersions in water–isopropanol mixtures. The amount of deposited material of the microporous layer was chosen so that the carbon black loading would be 1 mg/cm^2 of the GDL electrode area. After drying, active layers were deposited on the microporous layer.

Electrode active layers were also prepared by spraying from dispersions in water–isopropanol mixtures. The choice of a disperse medium for catalytic ink, i.e., water and isopropanol mixture (1 : 1 vol), was caused by fact that the PTFE powder used as a hydrophobisator material is well dispersed in such mixtures (at the same time, it actively coagulates in pure water and is moderately dispersed in pure isopropanol).

When preparing ink dispersions, the solid material concentration was, as a rule, 50–75 mg/ml. Ink components were mixed as follows. First, using an ultrasonic bath (PSB-Gals 5735-05m), a hydrophobisator was dispersed for no less than 10 min. Then the EC powder was poured with water and an equal isopropanol amount was added to the dispersion containing a hydrophobisator. Then there preparations were mixed, dispersed in the ultrasonic bath for a few minutes, diluted with the remaining water–isopropanol mixture, and sprayed by an aerograph on the GDL substrate with a preliminarily deposited microporous layer heated to 60°C.

In calculating the required amounts of ink components as a target platinum loading on the electrode surface, we proceeded from the number of 0.9 mg/cm^2 of the electrode area. This number was chosen because it corresponds to platinum contents on commercial electrodes produced by Pemeas/BASF, i.e., 0.9 mg/cm^2 of electrode area on the anode (pure platinum electrode, unlike the cathode). The loss during deposition reached 70%. After drying, electrodes were weighted, this value was compared with the mass of the GDL with the deposited microporous layer, and the platinum loading was determined.

One important and necessary phase of electrode preparation is annealing, which was performed in a muffle Barnstead Thermolyne High Temperature Furnace at a temperature of 350°C (above the PTFE hydrophobisator melting temperature of 320°C) for 20 min (except for furnace heating and cooling, which take about an hour) in an inert nitrogen atmosphere. Characteristics of unannealed electrodes at the same composition of active layers were significantly worse (by tens of mV at a current density of 0.4 A/cm^2 of electrode area). We explain this by the fact that comparatively large PTFE particles can form a well percolated system of gas-conducting channels with a high specific surface area in the AL structure only due to such annealing.

EC TESTING UNDER CONDITIONS OF OPERATING FC

Experimental Procedure

Characteristics of membrane-electrode assemblies (MEA) with an active area of 5 cm^2 were studied. The MEA consisted of sequentially packed layers, i.e., an anode, sealing gaskets, a doped phosphoric acid membrane, sealing gaskets, and a cathode. Sealing gaskets made of a PMF-A polyimide films (Estrokom, Russia) 120–130 μm thick and a film based on polyetheretherketone (Aptiv Co., Great Britain) 25–30 μm thick seal the electrode perimeter to prevent reagent leakage and fix the electrode active area. As an anode, we took an anode electrode from a commercial Pemeas Celtec P-1000 MEA with a platinum loading of 0.9 mg/cm^2 of the electrode area. The membrane (PBI matrix doped with phosphoric acid) was also taken from the commercial Pemeas Celtec P-1000 MEA. As cathodes, we took the prepared electrodes (see above) based on an EC synthesized in supercritical carbon dioxide with a platinum loading of ~0.9 mg/cm^2 of the electrode area.

The parameters of the FCs assembled using the EC synthesized in supercritical carbon dioxide were compared with reference characteristics of FCs assembled based on elements of standard commercial Pemeas Celtec P-1000 MEAs which currently exhibit record values of current–voltage characteristics [20, 21]. We note that, when assembling MEAs based on commercial Pemeas components, for a correct comparison, we took Pemeas anode electrodes for both the anode and cathode, since they are purely platinum with a loading of 0.9 mg/cm^2 of the electrode area, whereas Pemeas cathode electrodes contain Pt–Ni alloy [21].

The assembled FCs were put in stable operating conditions for 30–40 h (4–5 days for 8 h on average) by holding the under galvanostatic conditions at a load current of 0.4 A/cm^2 of the electrode area and a temperature of 160°C. Air and hydrogen were used as oxidizer and fuel; both reagents were fed without overpressure (relative to the atmospheric pressure).

The air flow was set significantly excessively in comparison with the stoichiometric one (the oxidizer supply stoichiometry is >5) to minimize diffusion limitations. The hydrogen flow slightly exceeded the stoichiometric one (the fuel supply stoichiometry is ≥2).

Current–voltage characteristics and impedance spectra were measured using a PGSTAT 302 (Eco Chemie B.V., Holland) potentiostat/galvanostat into which a module of a FRA2 frequency analyzer is incorporated. The FRA2 allows impedance measurements in a frequency range of 0.01 mHz–1 MHz. According to documentation, the current and potential measurement accuracy of the PGSTAT302 device is 0.2% of the current range limit and 0.2% of the potential value.

Analysis of Polarization Curves

Polarization curves were measured at a temperature of 160°C under galvanostatic conditions in the current range from 0 to 0.4 A/cm^2 of the electrode area with a current variation rate of 1 mA/(s cm^2 of the electrode area).

Cyclic Voltammetry

To estimate the crossover current, the standard chronocoulometry method [22] was used, for which a nitrogen flow was fed to the cathode, retaining the hydrogen flow to the anode, and a potential of 350 mV was set. About 10 min were taken for reaching a constant current, which corresponded to reaching a steady hydrogen flow from the anode to the cathode for oxidation (and chronocoulometry measurements); then the obtained crossover current estimate was fixed.

Thereafter, the accessible platinum surface in the cathode electrode was estimated. To this end, the nitrogen supply was disabled and cyclic voltammograms were measured. The potential was varied from 0 to 1.2 V with a rate of 100 mV/s. The desorption peak area was calculated and the total charge was determined and divided by 210 μC/cm^2 of the platinum area accessible for hydrogen adsorption, which allowed us to estimate the actual (electrochemically active) platinum surface in the cathode electrode [21, 24]. The two-electrode measurement geometry could slightly distort the measured values of the actual platinum surface; therefore, quantitatively, they could be characterized by a certain error; nevertheless, the obtained estimates can be undoubtedly used for a comparison of cathodes.

Impedometry

The impedance was measured under galvanostatic conditions at currents of 0.01, 0.02, 0.04, 0.12, 0.2, 0.28, 0.36, and 0.4 A/cm^2 of the electrode area in the frequency range of 40 kHz–0.5 Hz. The perturbing signal amplitude was 2 mA/cm^2 of the electrode area. After changing a load current, reaching the steady state was delayed for 15 min (in particular, to achieve steady-state amounts of water in the electrodes and membrane at a set certain current controlling the generation intensity on the cathode); then the impedance was measured. The impedance spectra were processed using the Origin 8 and Zview 3.1 programs.

RESULTS AND DISCUSSION

The main characteristics of ECs synthesized in the SC ÑÎ$_2$ medium are summarized in the table, including the results from data of their analysis using TEM and XRD.

Figure 1 shows the typical micrographs of obtained ECs and the corresponding size distributions of platinum particles. These electrocatalytic materials were then used to fabricate electrodes. One of the goals of the study was to develop a technique for producing electrocatalytic materials and verify its reproducibility. As the data from the table show, these goals were achieved. Indeed, a number of the electrocatalytic materials were synthesized which contain nanoscale particles of platinum on the carbon support with a narrow size distribution. Platinum particle sizes are reproducibly (from synthesis to synthesis) fitted into the range of 2–3 nm. Furthermore, it should be emphasized that the substrate nature (hydrophilic Vulcan XC72R or the more hydrophobic AS1 carbon black not subjected to any modification with the purpose of surface hydrophilization or hydrophobic nanotubes) have no effect on the metal particle morphology. Particle sizes according to TEM and crystallite sizes according to XRD are identical to characteristics of reference commercial materials HiSPEC3000 (20% Pt) and HiSPEC4000 (40% Pt) or exceed them (see table).

Characteristics of EC materials produced by synthesis in SC CO_2

Code	Support	Calculated Pt concentration, %	Measured Pt concentration, %	Pt particle size, nm (TEM)	Pt crystallite size (XRD)	Polydispersity factor (TEM)	Specific surface area, m^2/g (TEM)
HiSPEC 3000	Vulcan XC72R	20	19	2.1 ± 0.6	1.9 ± 0.1	2.0	110
HiSPEC 4000	Vulcan XC72R	40	38	2.8 ± 1.1	2.8 ± 0.1	1.7	80
N1	Vulcan XC72R	20	~10	2.0 ± 0.5	1.76 ± 0.13	1.6	120
N2	Vulcan XC72R	20	~19	1.7 ± 0.6	2.67 ± 0.15	3	130
N3	AS1	20	~18	1.8 ± 0.5	2.20 ± 0.14	1.7	130
N4	AS1	40	~38	2.3 ± 0.9	3.5 ± 0.4	3	90
N5	AS1	40	~36	2.4 ± 1.0	3.5 ± 0.5	6	80
N7	AS1	31	~31	2.0 ± 0.7	2.24 ± 0.14	3	110
N8	AS1	39	~38	2.2 ± 1.0	2.34 ± 0.11	2	90
N9a	AS1	30	~31	2.0 ± 0.8	1.86 ± 0.4	3	100
N9b	AS1	30	~31	1.9 ± 0.5	2.6 ± 0.4	1.7	130
N17	nanotubes	20	~21	2.4 ± 0.8	1.3 ± 0.1	2	100
N20	Vulcan XC72R	40	~40	2.3 ± 0.7	3.4	2	100
Z1	Vulcan XC72R	20	~12	1.7 ± 0.6	2.08 ± 0.04	2	130
Z2	Vulcan XC72R	23	~24	2.0 ± 0.6	1.88 ± 0.04	1.5	120

During the synthesis of catalytic materials (see the results of their morphology analysis in the table), we slightly varied thermal reduction conditions, in particular, the reduction temperature was 150–230°C; the inert medium for reduction was either an argon (pressure of 0.3–0.4 MPa) or carbon dioxide (6–30 MPa) atmosphere. The reduction time was unchanged (8 h). In this case, the reduction condition variation, in fact, had almost no effect on the achieved degree of monodispersity of platinum particles or on the uniformity of their distribution over the carbon support surface.

A comparison of the results of the table shows that the ECs synthesized by us are as good as commercial materials in their morphological properties. Currently, one of the main disadvantages of the developed approach associated with the use of SC CO_2 for synthesizing catalysts is the high cost of the technological cycle. Therefore, the major problem of the further development of this direction is reducing the cost of the developed technology. Among other factors, this includes searching for the possibility of reducing the cost of the materials. In particular, platinum complexes less expensive than $CODPt(CH_3)_2$ must be found. Here it is necessary to test other commercially available platinum precursors for their applicability to SC synthesis, which, being modified, can become soluble in SC CO_2. Of interest is the potential feasibility of impregnating the matrix with complexes insoluble

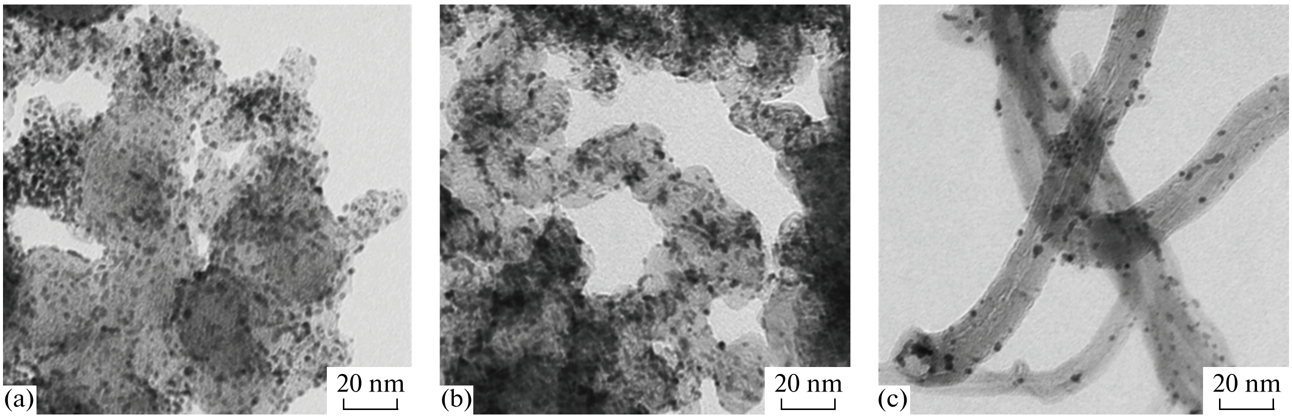

Fig. 1. Micrographs of electrocatalytic materials (left) and corresponding histograms of the size distribution of platinum particles (right) for ECs synthesized in the $SCCO_2$ medium: (a) sample Z2, ~24% Pt on Vulñan XC72R carbon black; (b) sample N9b, ~31% Pt on acetylene black AS1; sample N17, ~21% Pt on the surface of baytube C 150 HP nanotubes.

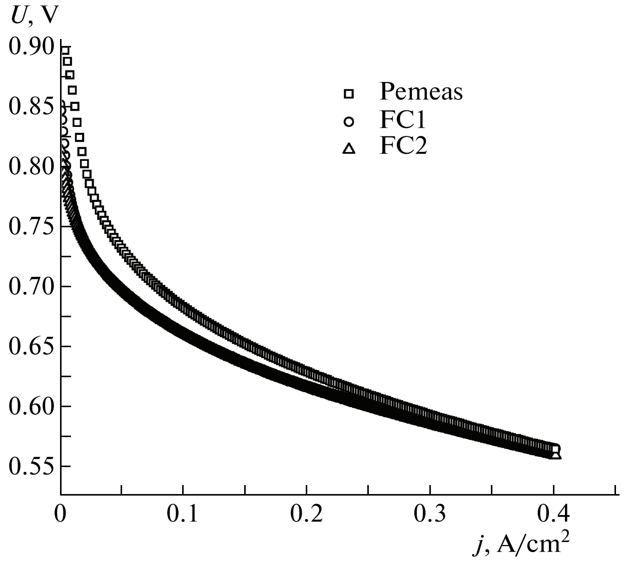

Fig. 2. Voltammograms of the phosphoric acid FC with cathode electrode fabricated with an EC synthesized under SC CO_2 conditions (FC1 and FC2 are, in fact, completely identical) in comparison with identically assembled FCs based on commercial BASF/Pemeas electrodes. Testing was performed at 160°C.

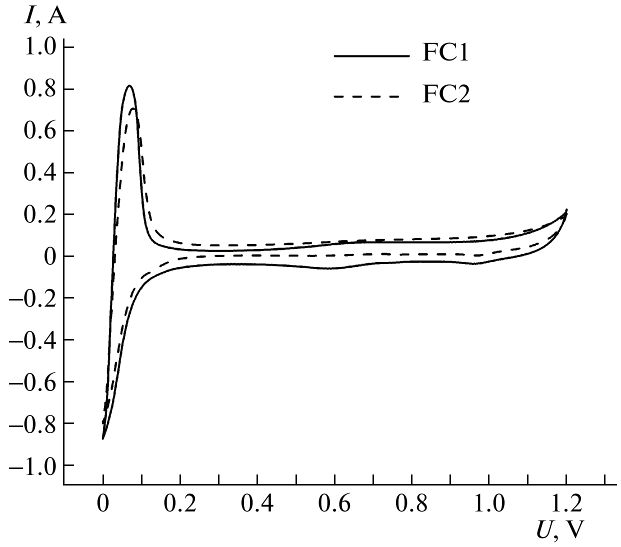

Fig. 3. Cyclic voltammograms for FC1 and FC2. The area under the curve in the hydrogen desorption region made it possible to estimate the actual (electrochemically active) platinum surface area per unit electrode area. Testing was performed at 160°C.

in SC CO_2, using surfactants and other dispersion stabilizers, e.g., water in SC CO_2. At the same time, even though it is more expensive than its analogues, the EC fabrication technology can become promising if the resulting materials have significantly better characteristics. Therefore, it was very important to test ECs synthesized by the SC technology as functional components of working electrochemical devices, i.e., the cathode electrodes of FCs.

When testing cathode electrodes fabricated based on the EC synthesized in SC CO_2 as a part of assembled FCs (FC1 and FC2), typical current–voltage characteristics were obtained (see Fig. 2). The obtained voltammograms were compared to characteristics of the reference FC assembled with commercial Pemeas electrodes.

A comparison (see Fig. 2) shows that FCs with electrodes based on ECs synthesized in SC CO_2 steadily show a lower open circuit voltage (OCV) than FCs based on Pemeas electrodes, i.e., 850 mV against 900–910 mV for Pemeas. However, the difference in the productivity disappears as the density of the current removed from the cell is approached, i.e., 0.4 A/cm^2 of the electrode area, which is considered the optimum operating point of this type of FC [20, 21].

To reveal the possible reasons for the lower OCVs for FCs with the original cathode electrode, it is reasonable to use the cyclic voltammetry method (see Fig. 3). For the actual platinum surface area per unit electrode surface area, we obtained values of 460, 380, and 600 (cm^2 of Pt area)/(cm^2 of the electrode area) for FC1, FC2, and Pemeas FCs, respectively. The crossover currents were, respectively, 2.4, 3.2, and 0.7 mA/cm^2 of the electrode area. The smaller area of the electrochemically active platinum surface in the prepared cathode electrodes when compared with commercial ones, in principle, could be explained by catalyst poisoning by the decomposition products of the organic precursor [25]. This hypothesis requires additional experimental verification by experiments with model platinum electrodes in phosphoric acid at 160°C in the presence of possible ligand fragments. However, the latter seems hardly probable, since electrodes were annealed at 350°C to melt dispersed PTFE in its composition, which should remove possible organic impurities (e.g., the boiling temperature of cyclooctadiene is 151°C). Therefore, we think that the most probable reason that the platinum surface in the electrodes we prepared is less active than commercial ones is the insufficient acid penetration into the porous structure of the active layer.

The more intense crossover currents detected for FCs with electrodes based on ECs synthesized in SC CO_2 probably explain the lower OCVs for them. Indeed, the very slow kinetics of the oxygen reaction in the presence of phosphoric acid results in a sharp dependence of the cathode potential of the phosphoric acid FC at low and zero external currents subtracted from internal currents, including crossover currents. Moreover, this sensitivity of the cathode overvoltage to crossover currents becomes more pronounced as the cathode exchange current decreases, which is proportional to the electrochemically active platinum surface [26, 27]. Since the measured electrochemically active platinum surface for cathode electrodes we prepared is lower and FCs on their basis are characterized by a larger detected crossover when compared with reference ones, the observed decrease in the OCV is quite expected. The increased crossover can be explained by the harder material of GDL electrodes prepared using ECs synthesized in SC CO_2 when compared to the GDLs of commercial electrodes (hard carbon paper against elastic carbon fabric). A harder electrode can perturb the structure of the comparatively soft PBI membrane matrix doped with phosphoric acid along the active region perimeter.

We note that, despite the significant difference (more than 50 mV) between OCVs, the productivity of all tested FCs at the standard reference point, i.e., at a taken current of 0.4 A/cm^2 of electrode area, is similar, i.e., 566, 560, and 566 mV for FC1, FC2, and Pemeas respectively. The current–voltage characteristics for FC1 and FC2 exhibit a smaller slope when compared with that of Pemeas almost in the entire current range.

The slope of the current–voltage characteristic, i.e., the differential internal resistance of the working FC, depends on the total loss within it, which is caused by the contributions of various processes (reagent diffusion, proton and electron transport under conditions of the existence of the ohmic resistances of the membrane and electrodes, electrode polarization during the charge transport in the electrochemical reaction, and others). In the absence of losses, corrosion currents of electrode materials, etc., the FC voltage would be controlled by equilibrium potentials and would be ~1.1 V at 160°C [21, 26, 27]. At low current densities, when the FC anode may be considered low-polarized, the FC voltage is controlled by cathode polarization. Even at low and zero currents, the cathode polarization is sufficiently high and, hence, is well described by the Tafel dependence [26], which can be presented in the form

$$j = i_0 \exp\left(\frac{\alpha_r F \eta}{RT}\right) - i_n, \tag{3}$$

where j is the current density through the electrode; i_0 is the cathode exchange current density; η is the deviation of the electrode potential from the equilibrium value (overvoltage); R is the universal gas constant; F is the Faraday constant; α_r is the transport coefficient; i_n is the sum of densities of all possible internal currents, i.e., the crossover currents, direct and shunting electron currents, currents of electrode material corrosion, etc. For an actual FC cathode, the relation $i_n \gg i_0$ is satisfied.

Although the Tafel equation itself describes only the polarization characteristic of the charge transfer stage, it is known that various portions of cathode polarization curves in the voltage–decimal logarithmic current density coordinates in experiments with FCs are often linear and are characterized by a constant slope which is either $b = RT\ln 10/\alpha_r F$ (a Tafel slope) or a double (or even quadruple) Tafel slope. As was discussed in the literature [28, 29], this change in the slope is caused not by a change in the oxygen reaction mechanism itself, but by the effect that mass transfer has on its rate.

The polarization curve slopes for assembled FCs were analyzed by impedance spectroscopy. The impedance was measured by the two-electrode method without a reference electrode. Thus, the measured impedance integrally includes both the cathode impedance of our interest and impedances of the membrane, anode, contacts, etc. The membrane impedance (with a possible contribution of impedance of contacts, GDLs, etc.) is generally believed to be equivalent to the simple ohmic resistance, which can be measured by the current break method [27] or by measuring the impedance at frequencies of 1–10 kHz [21, 24, 30]. In papers on phosphoric acid FCs, the anode impedance is generally assumed to be negligible in comparison with the cathode impedance [20, 21, 33], since the cathode is polarized much more strongly than the anode under conditions of testing of such FCs; as was estimated in [21], the anode polarization of the phosphoric acid FC with the PBI matrix is 4–5 mA at a current density of 0.4 A/cm^2, which is 100 times lower than the cathode polarization (400–500 mV) at the same current density. Based the results of theoretical studies [28, 29], the measured impedance spectra were analyzed in terms of the Tafel impedance,

$$Z_t = \frac{\tilde{\eta}}{\widetilde{\log(-j)}} = \ln 10 \frac{\tilde{\eta}}{\tilde{j}}(-j_{\mathrm{st}}) = -j_{\mathrm{st}} Z \ln 10 \tag{4}$$

The Tafel 1 impedance Z_t is defined as the ratio of the small perturbation of the electrode potential $\tilde{\eta}$ to the small perturbation of the decimal logarithmic current density $\widetilde{\log(-j)}$. Writing the current density j as the sum of the steady-state load current j_{st} and a the small perturbation current $\tilde{j}$, it is easy to find that the Tafel impedance Z_t is equal to the ordinary impedance Z multiplied by the density of the current of the load [28]. It is convenient to use the Tafel impedance, since its real part at low frequencies gives a local slope of the polarization characteristic in the voltage–decimal logarithmic current density coordinates [28, 33]. Comparing the obtained slope with the Tafel slope b, it is possible to make conclusions on processes limiting the FC productivity.

If the reaction is controlled only by the Tafel law, the obtained slope will be unchanged as the load current density increases and equal to the Tafel slope $b = RT\ln 10/\alpha_r F$. Under these conditions, we will observe semicircles of Tafel impedance spectra that are identical in diameter (with diameter $b = RT\ln 10/\alpha_r F$) for various current densities. However, if in the obtained slope is larger than b, according to the models of [28, 29], this will mean that limitations of mass

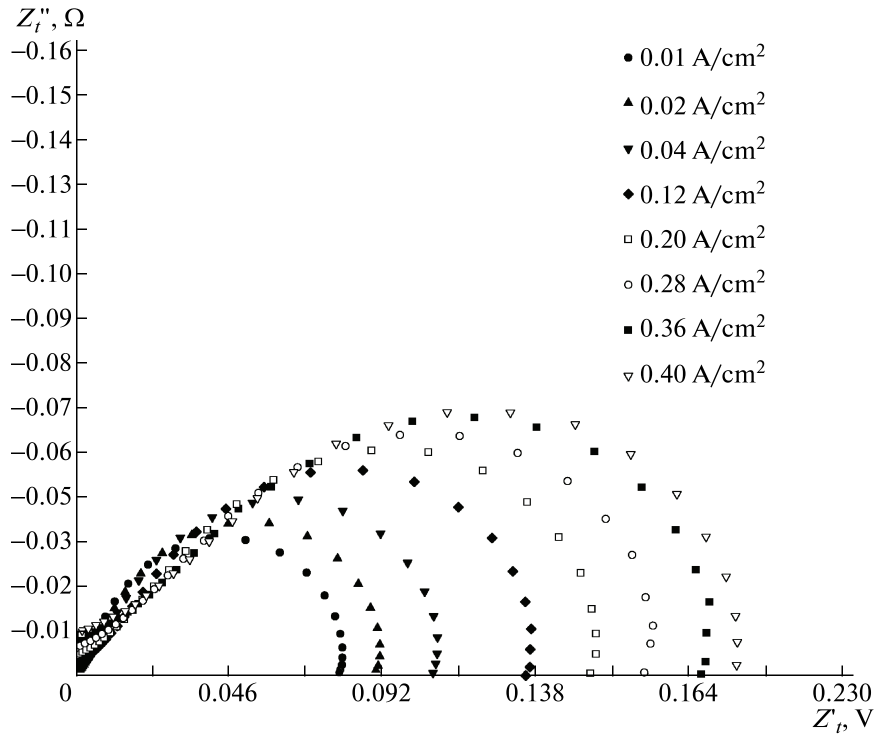

Fig. 4. Impedance spectra (corrected to the membrane ohmic resistance) of FCs with cathode electrode fabricated with an EC synthesized under SC CO_2 conditions.

transport processes in the cathode also affect the polarization curve (for example, along with the kinetics of the charge transport stages of the oxygen reaction, its rate becomes additionally controlled by oxygen diffusion in AL phosphoric acid, by proton migration in AL phosphoric acid electrolyte, or simultaneously by both factors).

For low current densities and strong air flows, the diffusion loss in the GDL can be neglected [30]. Then, among significant losses in the FC as a whole, only four basic mechanisms remain:

(i) kinetic and cathodic losses described by the Tafel law;

(ii) oxygen diffusion in the dissolved state in the catalytic layer of the cathode;

(iii) distributed ohmic losses in the cathode AL bulk caused by proton and electron transport;

(iv) ohmic losses in the membrane (undistributed ohmic losses).

As was noted above, the ohmic loss in the membrane (and, in principle, any other ohmic undistributed losses, including those in the GDL, in regions of electrode layer contacts, in regions of electrode–current collector contacts, etc.) can be easily accounted and excluded from consideration by measuring the impedance at high frequencies [21, 30] or using the current break method [27]. In this paper we set the membrane resistance equal to the real part of the impedance at a frequency of 10 kHz. The obtained resistances which we attributed to the ohmic loss in the membrane (their contribution to undistributed losses was estimated as the largest one) decrease with the current density and are ~0.1 Ω × cm^2 of the MEA active area, which is in good agreement with the published data on testing the MEA with the PBI matrix [21].

Figure 4 shows the Tafel impedance spectra corrected to ohmic losses for various current densities for FC1. For FC2, similar spectra were obtained. At low current densities (0.01 and 0.02 A/cm^2 of electrode area), the spectra are almost ideal semicircles with diameters of 0.078 and 0.087 V, respectively; i.e., the local slope at these current densities is 78 and 87 mV/dec, respectively, and is almost equal to the Tafel slope $b = RT\ln 10/\alpha_r F$ (85 mV/dec at a temperature of 160°C; in calculating the Tafel slope, we assumed that the transport coefficient α_r is unity according to Appleby's studies of the kinetics of the reaction of oxygen reduction in phosphoric acid [31] and in conventional practice to analyze polarization curves for phosphoric acid FCs with a PBI matrix [20, 21], where the observed Tafel slopes are about 2.3RT/F, which also corresponds to a transport coefficient α_r equal to unity). This value of the slope suggests that the cathode polarization at such low current densities is controlled by the oxygen reaction kinetics and is described by the Tafel equation, while oxygen diffusion and proton migration have no significant effect on the reaction rate [28, 32]. However, as the current den-

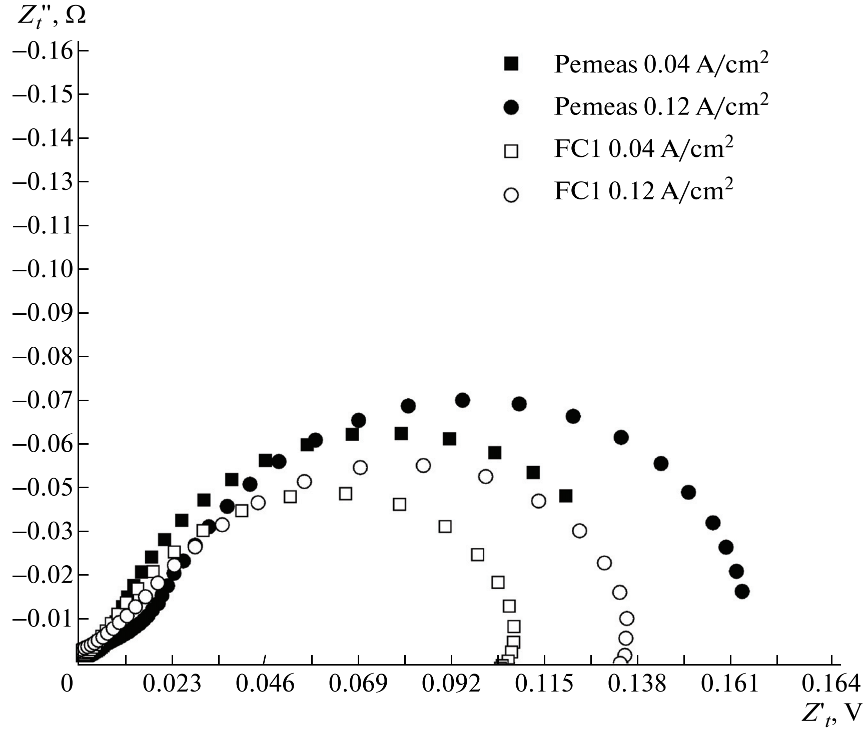

Fig. 5. Comparison of impedance spectra of FCs with cathode electrode fabricated with an EC synthesized under SC CO_2 conditions and FCs based on commercial Pemeas/BASF electrodes.

sity increases, a characteristic 45ˆ slope appears in the high-frequency region of the spectra (this slope was repeatedly described in the literature, see, e.g., [30, 32], where it is easily seen even from 0.12 A/cm^2 of electrode area), and the Tafel impedances at low frequencies on the real axis increase to 196 mV/dec (more than 2b) at a current of 0.4 A/cm^2 of electrode area. This 45° slope in the high-frequency region appears due to the distributed resistance in the cathode active layer bulk, which is caused mainly by proton transport in the active layer [28, 30, 33]. According to [28, 29, 32], the polarization curve slope exceeding 2b in the voltage–decimal logarithmic current density coordinates is observed if the processes limiting FC productivity are simultaneously the kinetic polarization, proton migration, and oxygen diffusion in the active layer.

A qualitatively similar pattern is also observed for FCs based on commercial Pemeas electrodes; i.e., mass transport limitations at higher current densities begin to affect the cathode polarization as well. However, one significant difference is that the characteristic 45° slope in the high-frequency spectral region for FCs based on Pemeas electrodes is more pronounced even at lower current densities. Furthermore, the local slopes of polarization curves in the voltage–decimal logarithmic current density coordinates, as determined from the impedance for Pemeas-based FCs, are larger than the slopes for FC1 and FC2 at the same current densities (see Fig. 5). In this case, as was noted above, cyclic voltammetry measurements showed that the actual platinum surface in FCs based on Pemeas electrodes is larger than that in FC1 and FC2 with ECs synthesized under SC CO_2 conditions. This means that the transition to conditions with the polarization characteristic slope increased over *b* in FCs based on Pemeas electrodes occurs at significantly lower currents per unit platinum surface area than for FC1 and FC2. Therefore, it is clear that the transition to larger slopes is apparently unrelated to a change in the mechanism of the multistage reaction of oxygen reduction, but it is caused exactly by the effect of transport limitations in the catalytic layer bulk (mostly by proton migration and oxygen diffusion) [28, 29], which are more pronounced in Pemeas electrodes and begin to appear at lower current densities.

It seems that the transport processes in the cathode electrodes developed based on electrocatalytic materials synthesized in SC CO_2 associated with oxygen diffusion in the active layer partially flooded with phosphoric acid and charge migration (with protons in phosphoric acid electrolyte partially filling the active layer and electrons in dispersed percolated structures of carbon material) are more efficient, which is probably caused by the detected uniformity of the distribution of comparatively monodisperse platinum particles on the carbon substrate.

In addition, it should be noted that the high degree of monodispersity of platinum particles produced by the method developed in this study allows us to expect good resource characteristics of the catalytic material during its long-term operation in phosphoric acid FCs due to the suppressed Ostwald ripening mechanism.

CONCLUSIONS

Thus, reproducible laboratory technology for synthesizing ECs in the SC CO_2 medium was developed which makes it possible to produce monodisperse nanoscale platinum particles on a carbon substratum regardless of the degree of its surface hydrophily. The sizes of the particles and the platinum specific surface area, including the electrochemically active one, for synthesized ECs are highly competitive with the characteristics of the best commercial materials of the Johnson–Matthey Company, i.e., HiSPEC3000 and HiSPEC4000.

Testing ECs under conditions of an operating FC showed a significant decrease in limitations to mass transport processes in the active layer bulk (oxygen diffusion and proton migration) of the electrode containing these materials when compared with the electrode of the currently most efficient commercial Pemeas Celtec P-1000 MEA.

ACKNOWLEDGMENTS

The authors are grateful to Assoc. Prof. S.S. Abramchuk for an analysis of ECs by TEM, scientific associate E.E. Levin for XRD studies, and Profs. P.M. Valetskii and A.S. Kotosonov for the acetylene black AB1 samples put at their disposal.

This study was supported by the Federal target program "Scientific and Pedagogical Personnel of an Innovative Russia" for 2009–2013 (state contract P924).

REFERENCES

1. J. J. Watkins and T. J. McCarthy, "Polymer/Metal Nanocomposite Synthesis in Supercritical CO_2," Chem. Mater. **7** (11), 1991–1994 (1995).
2. E. N. Sobol, V. N. Bagratashvili, V. K. Popov, A. E. Sobol, E. E. Said-Galiev, and L. N. Nikitin, "Kinetics of Diffusion of Metalloorganic Compounds in Polymers from Supercritical CO_2 Solutions," Zh. Fiz. Khim. **72** (1), 28–31 (1998) [Russ. J. Phys. Chem. A **72** (1), 23–26 (1998)].
3. E. N. Sobol', V. N. Bagratashvili, A. E. Sobol', and S. M. Howdle, "Kinetics of Polymer Impregnation in Supercritical Media," Dokl. Akad. Nauk **356** (4–6), 777–780 (1997) [Dokl. Phys. Chem. **356** (4–6), 346–348 (1997)].
4. C. Erkey, "Preparation of Metallic Supported Nanoparticles and Films Using Supercritical Fluid Deposition," J. Supercrit. Fluids **47**, 517–522 (2009).
5. P. H. Tewari, A. J. Hunt, and K. D. Lofftus, "Ambient-Temperature Supercritical Drying of Transparent Silica Aerogels," Mater. Lett. **3** (9–10), 363–367 (1985).
6. N. E. Fernandes, S. M. Fisher, J. C. Poshusta, D. G. Vlachos, M. Tsapatsis, and J. J. Watkins, "Reactive Deposition of Metal Thin Films within Porous Supports from Supercritical Fluids," Chem. Mater. **13** (6), 2023–2031 (2001).
7. A. I. Cooper, "Recent Developments in Materials Synthesis and Processing Using Supercritical CO_2," Adv. Mater. (Weinheim) **13** (14), 1111–1114 (2001).
8. Y. Zhang, D. Kang, C. Saquing, M. Aindow, and C. Erkey, "Supported Platinum Nanoparticles by Supercritical Deposition," Ind. Eng. Chem. Res. **44** (11), 4161–4164 (2005).
9. Y. Zhang and C. Erkey, "Preparation of Platinum–Nafion–Carbon Black Nanocomposites via a Supercritical Fluid Route as Electrocatalysts for Proton Exchange Membrane Fuel Cells," Ind. Eng. Chem. Res. **44** (14), 5312–5317 (2005).
10. Y. Zhang and C. Erkey, "Preparation of Supported Metallic Nanoparticles Using Supercritical Fluids: A Review," J. Supercrit. Fluids **38** (2), 252–267 (2006).
11. C. H. Yen, K. Shimizu, Y.-Y. Lin, F. Bailey, I. F. Cheng, and C. M. Wai, "Chemical Fluid Deposition of Pt-Based Bimetallic Nanoparticles on Multiwalled Carbon Nanotubes for Direct Methanol Fuel Cell Application," Energy Fuels **21** (4), 2268–2271 (2007).
12. W. Zhou and J. Y. Lee, "Highly Active Core–Shell Au@Pd Catalyst for Formic Acid Electrooxidation," Electrochem. Commun. **9** (7), 1725–1729 (2007).
13. A. Bayrakceken, A. Smirnova, U. Kitkamthorn, M. Aindow, L. Türker, I. Erolu, and C. Erkey, "Pt-Based Electrocatalysts for Polymer Electrolyte Membrane Fuel Cells Prepared by Supercritical Deposition Technique," J. Power Sources **179** (2), 532–540 (2008).
14. H. Zhao, L. Li, J. Yang, and Y. Zhang, "Co@Pt–Ru Core–Shell Nanoparticles Supported on Multiwalled Carbon Nanotube for Methanol Oxidation," Electrochem. Commun. **10** (10), 1527–1529 (2008).
15. Y. Zhang, B. Cangul, Y. Garrabos, and C. Erkey, "Thermodynamics and Kinetics of Adsorption of Bis(2,2,6,6-Tetramethyl-3,5-Heptanedionato) (1,5-Cyclooctadiene) Ruthenium(II) on Carbon Aerogel from Supercritical CO_2 Solution," J. Supercrit. Fluids **44** (1), 71–77 (2008).
16. B. Cangul, L. C. Zhang, M. Aindow, and C. Erkey, "Preparation of Carbon Black Supported Pd, Pt, and Pd–Pt Nanoparticles Using Supercritical CO_2 Deposition," J. Supercrit. Fluids **50** (1), 82–90 (2009).
17. M.-K. Min, J. Cho, K. Cho, and H. Kim, "Particle Size and Alloying Effects of Pt-Based Alloy Catalysts for Fuel Cell Applications," Electrochim. Acta **45** (25–26), 4211–4217 (2000).
18. N. P. Lebedeva, M. T. M. Koper, J. M. Feliu, and R. A. van Santen, "Role of Crystalline Defects in Electrocatalysis: Mechanism and Kinetics of CO Adlayer Oxidation on Stepped Platinum Electrodes," J. Phys. Chem. B **106** (50), 12938–12947 (2002).
19. F. Maillard, S. Schreier, M. Hanzlik, E. R. Savinova, S. Weinkauf, and U. Stimming, "Influence of Particle Agglomeration on the Catalytic Activity of Carbon-Supported Pt Nanoparticles in CO Monolayer Oxidation," Phys. Chem. Chem. Phys **7**, 385–393 (2005).

20. T. J. Schmidt and J. Baurmeister, "Properties of High-Temperature PEFC Celtec®-P 1000 MEAs in Start/Stop Operation Mode," J. Power Sources **176** (2), 428–434 (2008).
21. K. C. Neyerlin, A. Singh, and D. Chu, "Kinetic Characterization of a Pt–Ni/C Catalyst with a Phosphoric Acid Doped PBI Membrane in a Proton Exchange Membrane Fuel Cell," J. Power Sources **176** (1), 112–117 (2008).
22. M. Inaba, T. Kinumoto, M. Kiriake, R. Umebayashi, A. Tasaka, and Z. Ogumi, "Gas Crossover and Membrane Degradation in Polymer Electrolyte Fuel Cells," Electrochim. Acta **51**, 5746–5753 (2006).
23. Z. Qi and S. Buelte, "Effect of Open Circuit Voltage on Performance and Degradation of High-Temperature PBI–H_3PO_4 Fuel Cells," J. Power Sources **161** 1126–1132 (2006).
24. J. Zhang, Y. Tang, C. Song, and J. Zhang, "Polybenzimidazole-Membrane-Based PEM Fuel Cell in the Temperature Range of 120–200°C," J. Power Sources **172** 163–171 (2007).
25. E. E. Said-Galiyev, A. Yu. Nikolaev, E. E. Levin, E. K. Lavrentyeva, M. O. Gallyamov, S. N. Polyakov, G. A. Tsirlina, O. A. Petrii, and A. R. Khokhlov, "Structural and Electrocatalytic Features of Pt/C Catalysts Fabricated in Supercritical Carbon Dioxide," J. Solid State Electrochem. **15** (3), 623–633 (2011).
26. S. M. Haile, "Fuel Cell Materials and Components," Acta Mater. **51**, 5981–6000 (2003).
27. J. Larminie and A. Dicks, *Fuel Cell Systems Explained*, 2nd ed. (Wiley, Chichester, 2003).
28. F. Jaouen and G. Lindbergh, "Transient Techniques for Investigating Mass-Transport Limitations in Gas Diffusion Electrodes: I. Modeling the PEFC Cathode," J. Electrochem. Soc. **150** (12), A1699–A1710 (2003).
29. F. Jaouen, G. Lindbergh, and G. Sundholm, "Investigation of Mass-Transport Limitations in the Solid Polymer Fuel Cell Cathode: I. Mathematical Model," J. Electrochem. Soc. **149** (4), A437 (2002).
30. R. Makharia, M. F. Mathias, and D. R. Baker, "Measurement of Catalyst Layer Electrolyte Resistance in PEFCs Using Electrochemical Impedance Spectroscopy," J. Electrochem. Soc. **152** (5), A970–A977 (2005).
31. A. J. Appleby, "Oxygen Reduction on Oxide-Free Platinum in 85% Orthophosphoric Acid: Temperature and Impurity Dependence," J. Electrochem. Soc. **177** (3), 328–335 (1970).
32. F. Jaouen, G. Lindbergh, and K. Wiezell, "Transient Techniques for Investigating Mass-Transport Limitations in Gas Diffusion Electrodes: II. Experimental Characterization of the PEFC Cathode," J. Electrochem. Soc. **150** (12), A1711–A1717 (2003).
33. E. Springer, A. Zawodzinski, M. S. Wilson, and S. Golfesfeld, "Characterization of Polymer Electrolyte Fuel Cells Using AC Impedance Spectroscopy," J. Electrochem. Soc. **143** (2), 587–599 (1996).

SPELL OK